



Research

Cite this article: Cakoni F, Haddar H, Zilberberg D. 2024 An algorithm for computing scattering poles based on dual characterization to interior eigenvalues. *Proc. R. Soc. A* **480**: 20240015. <https://doi.org/10.1098/rspa.2024.0015>

Received: 6 January 2024

Accepted: 21 May 2024

Subject Areas:

applied mathematics, analysis

Keywords:

inverse scattering, obstacle scattering, scattering poles, resonances

Author for correspondence:

Fioralba Cakoni

e-mail: fc292@math.rutgers.edu

One contribution to a special feature 'Mathematical theory and applications of multiple wave scattering' organized by guest editors Luke G. Bennetts, Michael H. Meylan, Malte A. Peter, Valerie J. Pinfield and Olga Umnova.

THE ROYAL SOCIETY
PUBLISHING

An algorithm for computing scattering poles based on dual characterization to interior eigenvalues

Fioralba Cakoni¹, Houssem Haddar³ and

Dana Zilberberg²

¹Department of Mathematics, and ²Department of Mathematics, Rutgers University, New Brunswick, NJ, USA

³INRIA, UMA, ENSTA Paris, Institut Polytechnique de Paris, Palaiseau, France

FC, 0000-0002-4648-8780

We present an algorithm for the computation of scattering poles for an impenetrable obstacle with Dirichlet or Robin boundary conditions in acoustic scattering. This paper builds upon the previous work of Cakoni *et al.* (2020) titled 'A duality between scattering poles and transmission eigenvalues in scattering theory' (Cakoni *et al.* 2020 *Proc. A.* **476**, 20200612 ([doi:10.1098/rspa.2020.0612](https://doi.org/10.1098/rspa.2020.0612))), where the authors developed a conceptually unified approach for characterizing the scattering poles and interior eigenvalues corresponding to a scattering problem. This approach views scattering poles as dual to interior eigenvalues by interchanging the roles of incident and scattered fields. In this framework, both sets are linked to the kernel of the relative scattering operator that maps incident fields to scattered fields. This mapping corresponds to the exterior scattering problem for the interior eigenvalues and the interior scattering problem for scattering poles. Leveraging this dual characterization and inspired by the generalized linear sampling method for computing the interior eigenvalues, we present a novel numerical algorithm for computing scattering poles without relying on an iterative scheme. Preliminary numerical examples showcase the effectiveness of this computational approach.

1. Introduction

The theory of scattering poles, also referred to as resonances, constitutes a rich and beautiful aspect of scattering theory. For an extensive exploration of the subject, we direct the reader to the monograph [1]. The concept of scattering poles is inherently dynamic, as it captures physical information about waves by associating the rate of oscillations with the real part of a pole and the rate of decay with its imaginary part. However, an elegant mathematical formulation arises when considering them as the poles of the meromorphic extension of the scattering operator [2,3]. For a broad class of scattering problems, it is known that scattering poles exist and are complex with negative imaginary parts. Various properties of scattering poles, such as estimates of their density and bounds for obstacle scattering or inhomogeneous media, including dissipative systems, can be found in the literature (e.g. [4–11]; this list is by no means exclusive). Numerical methods for computing scattering poles have also been proposed in the literature (e.g. [12–14] and references therein). Scattering poles have been proposed as a tool for solving the inverse scattering problem, and radar identification often relies on the study of these resonant frequencies [15,16]. Uniqueness and stability results for recovering impenetrable obstacles from knowledge of scattering poles have been proven, as seen in [6,17,18]. However, a practical challenge associated with inverse scattering is the difficulty in measuring the scattering poles, as they are complex while the interrogating frequency in an experiment is real.

At a scattering pole, there is a non-zero scattered field in the absence of the incident field. This property precisely enables the capturing of scattering poles as an eigenvalue problem. On the flip side of this characterization of scattering poles, one might inquire whether there are frequencies for which an incident field exists that does not scatter due to the scattering object. The answer to this question leads to an interior eigenvalue problem associated with the support of the scatterer. In the case of scattering by a bounded impenetrable obstacle, such as with Dirichlet boundary conditions, this is simply the Dirichlet eigenvalue problem for a symmetric elliptic operator. A more intriguing situation arises in the scattering by an inhomogeneous medium where a new eigenvalue problem emerges, referred to as the transmission eigenvalue problem [19]. This is a non-self-adjoint eigenvalue problem formulated in the support of inhomogeneity for two homogeneous elliptic partial differential equations sharing the same Cauchy data. Exploiting mathematically the fact that at an interior eigenvalue, there are normalized incident fields that produce arbitrarily small scattered fields, it is possible to show that the interior eigenvalues can be determined from the (measured) relative scattering operator corresponding to the physical scattering experiment [19–21]. This analysis has led to computable algorithms for determining the interior eigenvalues by the generalized linear sampling method (GLSM) in inverse scattering theory [19,22]. In order to transfer these techniques to the computation of scattering poles, the authors in [23] introduced a duality argument between scattering poles and interior eigenvalues for a Dirichlet obstacle and an inhomogeneous medium of bounded support. In particular, the scattering poles are studied in connection with the kernel of an operator that plays the same role as the relative scattering operator in relation to the Dirichlet eigenvalues and transmission eigenvalues, respectively. This duality is revealed by flipping the roles of interior and exterior domains and has led to a new way of defining the scattering poles. However, [23] fell short of turning this new characterization into a computable algorithm. Our current paper can be seen as a continuation of [23], with the main goal being to develop and implement an algorithm for computing the scattering poles based on this dual characterization using the GLSM.

Our paper is organized as follows. In §2, we summarize the analytical results obtained in [23] regarding the duality between the scattering poles for a Dirichlet obstacle and the corresponding Dirichlet eigenvalues. Based on these results, we derive the GLSM, leading to an implementable algorithm for computing the scattering poles. We then outline a particular implementation procedure in the two-dimensional case. In §3, we develop the theory for the duality of the scattering poles for an impedance obstacle (also known as an obstacle with Robin boundary conditions) and the corresponding impedance eigenvalues. This aspect was not included in [23], and here in addition, we provide a GLSM computational algorithm. The

Robin boundary conditions model the scattering by an impenetrable scatterer coated with a thin layer of lossy and/or dispersive material. Section 4 presents a preliminary numerical study. Although not included here, our algorithm can be used to compute the scattering poles for an inhomogeneous medium of bounded support (possibly absorbing and dispersive) based on the analysis developed in [23]. We emphasize that our algorithm for computing the scattering poles is universal for any physical scattering problem involving bounded scatterers, provided that the interior scattering operator is given. To compute the interior scattering operator, one uses the model governing the scattering phenomenon through the solution of the interior scattering problem. Regarding the use of scattering poles in inverse scattering problems, a primary concern of our method is whether access to the interior scattering operator is feasible, either experimentally or computationally, based on scattering measurements.

2. Scattering poles for a Dirichlet obstacle

Let D be a bounded simply connected region in \mathbb{R}^m ($m = 2, 3$) with Lipschitz boundary ∂D . We denote by ν the outward unitary normal vector on ∂D . The scattering problem for a Dirichlet obstacle is formulated as: given an incident field v which is solution of the Helmholtz equation $\Delta v + k^2 v = 0$ in \mathbb{R}^m (except for possibly a subset of measure zero in the exterior of D), find the scattered field $u^s \in H^1_{\text{loc}}(\mathbb{R}^m \setminus D)$ such that

$$\begin{aligned} \Delta u^s + k^2 u^s &= 0 \quad \text{in } \mathbb{R}^m \setminus \bar{D} \\ u^s &= -v \quad \text{on } \partial D \\ \lim_{r \rightarrow \infty} r^{(m-1)/2} \left(\frac{\partial u^s}{\partial r} - iku^s \right) &= 0. \end{aligned} \tag{2.1}$$

This problem is well-posed for $k \in \mathbb{C}$ with $\Im(k) \geq 0$. Let $B \subset \mathbb{R}^m$ be a bounded region such that $D \subset B$ with Lipschitz boundary ∂B , and consider incident waves $v := v_g$ which are superposition of point sources located at $y \in \partial B$ (otherwise referred to as surface potential) given by

$$v_g(x) = \int_{\partial B} g(y) \Phi_k(x, y) \, ds(y), \tag{2.2}$$

where $\Phi_k(\cdot, \cdot)$ is the fundamental solution of the Helmholtz equation defined by

$$\Phi_k(x, y) := \frac{i}{4} H_0^{(1)}(k|x - y|) \quad \text{for } m = 2 \quad \text{and} \quad \Phi_k(x, y) = \frac{e^{ik|x-y|}}{4\pi|x - y|} \quad \text{for } m = 3.$$

By linearity of the direct scattering problem, the corresponding scattered field $u^s := u_g^s$ is given by

$$u_g^s(x) = \int_{\partial B} g(y) u^s(x, y) \, ds(y), \tag{2.3}$$

where $u^s(\cdot, y)$ is the scattered field due to a point source located at $y \in \partial B$, i.e. $u^s(\cdot, y)$ solves (2.1) with $v := \Phi(\cdot, y)$. In this framework, we define the relative scattering operator (aka near field operator) $\mathcal{S}_k : L^2(\partial B) \rightarrow L^2(\partial B)$ mapping

$$\mathcal{S}_k : g \mapsto u_g^s|_{\partial B}, \tag{2.4}$$

where u_g^s is given by (2.3). The interior eigenvalues arise from the study of the injectivity of the relative scattering operator $\mathcal{S}_k g = 0$, in other words looking for an incident field v_g that does not scatter by the Dirichlet obstacle D . One can easily check that $\mathcal{S}_k g = 0$ if k is a Dirichlet eigenvalue of the negative Laplacian in D and with corresponding eigenfunction of the form given by (2.2). We call such k non-scattering wave numbers. In general, the Dirichlet eigenfunction is defined only in D , and may not even be extendable outside D as solution of the Helmholtz equation. Therefore, not all Dirichlet eigenvalues are non-scattering wavenumbers. In order to explore further this

connection of Dirichlet eigenvalues with non-scattering wavenumbers, we consider the forward problem with more general Dirichlet data, namely

$$\begin{aligned} \Delta w + k^2 w &= 0 && \text{in } \mathbb{R}^m \setminus \bar{D} \\ w &= -v && \text{on } \partial D \\ \lim_{r \rightarrow \infty} r^{(m-1)/2} \left(\frac{\partial w}{\partial r} - ikw \right) &= 0, \end{aligned} \quad (2.5)$$

where $v \in H_{\text{inc}}(D)$ defined by

$$H_{\text{inc}}(D) := \{v \in H^1(D) : \Delta v + k^2 v = 0\} \text{ equipped with } H^1(D)\text{-norm.}$$

We obviously have

$$\mathcal{S}_k g = -\mathcal{W}_k \mathcal{H}g,$$

where

$$\mathcal{W}_k : v \in H_{\text{inc}}(D) \mapsto w|_{\partial B} \in L^2(\partial B),$$

with w solving (2.5)

$$\text{and } \mathcal{H} : g \mapsto v_g|_D, L^2(\partial B) \rightarrow H^{\text{inc}}(D).$$

Hence $\mathcal{W}_k v = 0$ if and only if k is a Dirichlet eigenvalue with v the corresponding eigenfunctions. Since $\{\mathcal{H}g, g \in L^2(\partial B)\}_{H^1(D)} = H_{\text{inc}}(D)$ [23, Lemma 2.7], we can conclude that $k \in \mathbb{R}$ is a Dirichlet eigenvalue if and only if there exists a sequence of $g_j \in L^2(\partial B)$ such that the sequence $\mathcal{H}g_j$ converges to a non-zero $v \in \text{Kern } \mathcal{W}_k$ in $H^1(D)$ -norm. The above characterization of Dirichlet eigenvalues is used to compute them merely from a knowledge of the relative scattering operator \mathcal{S}_k using the linear sampling and generalized linear sampling methods [19,20].

In [23, Section 2], a similar characterization of the scattering poles in terms of the kernel of a new scattering operator is introduced, which can be viewed as dual to the above characterization of the Dirichlet eigenvalues. Indeed, let us denote by j_ℓ the spherical Bessel function of order ℓ , by $h_\ell^{(1)}$ the spherical Hankel function of the first kind of order ℓ , and by Y_ℓ a spherical harmonic of order ℓ (see [24, Section 2.3, §2.4]). If we consider the scattering of $v = j_\ell(k|x|)Y_\ell(\hat{x})$ (which is a superposition of point sources located at infinity) by a Dirichlet ball of radius one in \mathbb{R}^3 we have that the Dirichlet eigenvalues are the zeros of $j_\ell(k) = 0$ (for such k , $j_\ell(k|x|)Y_\ell(\hat{x})$ is the corresponding eigenfunction), where the scattering poles are the zeros of $h_\ell^{(1)}(k) = 0$. We note that $h_\ell^{(1)}(k|x|)Y_\ell(\hat{x})$ are superposition of point sources located at the origin [24]. This duality motivates the consideration of an appropriate interior scattering problem inside D which will be the basis of our characterization of scattering poles in the similar but dual to the Dirichlet eigenvalues stated above. For the sake of the reader's convenience in the following, we sketch this construction in [23, Section 2] and summarize the main theoretical results, which will be the basis of our computational algorithm.

To this end, for a generic $m - 1$ dimensional closed Lipschitz manifold $\partial \mathcal{O}$ enclosing a bounded region \mathcal{O} , we recall the definition of the single-layer potential $\text{SL}_{\partial \mathcal{O}}^k : H^{s-1/2}(\partial \mathcal{O}) \rightarrow H_{\text{loc}}^{s+1}(\mathbb{R}^m \setminus \partial \mathcal{O})$ (see [25] for the mapping properties)

$$\text{SL}_{\partial \mathcal{O}}^k(\psi)(x) := \int_{\partial D} \psi(y) \Phi_k(x, y) \, ds_y, \quad x \in \mathbb{R}^m \setminus \partial \mathcal{O}, \quad (2.6)$$

and double layer potential $\text{DL}_{\partial \mathcal{O}}^k : H^{s+1/2}(\partial \mathcal{O}) \rightarrow H_{\text{loc}}^{s+1}(\mathbb{R}^m \setminus \partial \mathcal{O})$

$$\text{DL}_{\partial \mathcal{O}}^k(\psi)(x) := \int_{\partial \mathcal{O}} \psi(y) \frac{\partial \Phi_k(x, y)}{\partial \nu_y} \, ds_y, \quad x \in \mathbb{R}^m \setminus \partial \mathcal{O}, \quad (2.7)$$

where $-1 \leq s \leq 1$ (this is the range for Lipschitz $\partial \mathcal{O}$, for smooth manifold the above mapping properties hold for larger $|s|$).

One then can prove that the scattering problem (2.5) is equivalent to seeking $w \in H_{\text{loc}}^1(\mathbb{R}^m \setminus D)$ such that

$$\begin{cases} \Delta w + k^2 w = 0 & \text{in } \mathbb{R}^m \setminus \bar{D} \\ w = f & \text{on } \partial D \\ w = \text{SL}_{\partial D}^k \left(\frac{\partial w}{\partial \nu} \right) - \text{DL}_{\partial D}^k(w) & \text{in } \mathbb{R}^m \setminus \bar{D}, \end{cases} \quad (2.8)$$

which again has a unique solution for $k \in \mathbb{C}$ with $\Im(k) \geq 0$. This formulation allows us to define the scattering poles.

Definition 2.1. $k \in \mathbb{C}$ is a scattering pole of the Dirichlet scattering problem for D if the homogeneous problem (2.8), i.e. with $f = 0$, has a non-trivial solution.

This definition is equivalent to the one given in [26, Theorem 7.11]. It is well known that these scattering poles lie in the complex lower half-plane $\mathbb{C}_- := \{z \in \mathbb{C}, \Im(z) < 0\}$ and form a discrete set without accumulation points. The dual notion mentioned above for the case of a ball motivated the introduction of the following interior scattering problem. Assume that $k > 0$ is not a Dirichlet eigenvalue (since we are interested in the scattering poles which are complex this assumption does not present any restrictions). Then for a point $z \in D$, let $u^s(\cdot, z) \in H^1(D)$ be the unique solution of

$$\begin{cases} \Delta u^s(\cdot, z) + k^2 u^s(\cdot, z) = 0 & \text{in } D \\ u^s(\cdot, z) = -\Phi_k(\cdot, z) & \text{on } \partial D. \end{cases} \quad (2.9)$$

Next consider a region $\mathcal{C} \subset D$ in \mathbb{R}^m inside D with smooth Lipschitz boundary $\partial \mathcal{C}$ and define the interior scattering operator $\mathcal{N}_k : L^2(\partial \mathcal{C}) \rightarrow L^2(\partial \mathcal{C})$

$$\mathcal{N}_k \varphi(x) = \int_{\partial \mathcal{C}} \varphi(z) u^s(x, z) \, ds(z), \quad x \in \partial \mathcal{C}. \quad (2.10)$$

The operator \mathcal{N}_k is compact, symmetric (see [23, Lemma 2.5]) and maps

$$\mathcal{N}_k : \varphi \mapsto u_\varphi^s|_{\partial \mathcal{C}}, \quad (2.11)$$

where $u_\varphi^s \in H^1(D)$ is the unique solution of

$$\begin{cases} \Delta u_\varphi^s + k^2 u_\varphi^s = 0 & \text{in } D \\ u_\varphi^s = -\text{SL}_{\partial \mathcal{C}}^k(\varphi) & \text{on } \partial D \end{cases} \quad (2.12)$$

and

with $\text{SL}_{\partial \mathcal{C}}^k(\varphi)$ given by (2.6). The scattering poles are related to the injectivity of \mathcal{N}_k , which plays the same role that S_k plays with respect to the Dirichlet eigenvalues. More precisely, let us define the space of exterior incident fields

$$H_{\text{inc}}^e(D) := \{w \in H_{\text{loc}}^1(\mathbb{R}^m \setminus D), w \text{ satisfies (2.14)}\} \quad (2.13)$$

and

$$\begin{cases} \Delta w + k^2 w = 0 & \text{in } \mathbb{R}^m \setminus \bar{D} \\ w = \text{SL}_{\partial D}^k \left(\frac{\partial w}{\partial \nu} \right) - \text{DL}_{\partial D}^k(w) & \text{in } \mathbb{R}^m \setminus \bar{D}. \end{cases} \quad (2.14)$$

This space can be equipped with the norm

$$\|w\|_{H_{\text{inc}}^e(D)} := \left(\|w\|_{H^{1/2}(\partial D)}^2 + \left\| \frac{\partial w}{\partial \nu} \right\|_{H^{-1/2}(\partial D)}^2 \right)^{1/2}.$$

We define the operator $\mathcal{G}_k : H_{\text{inc}}^e(D) \rightarrow L^2(\partial \mathcal{C})$ as the mapping $w \mapsto u_w|_{\partial \mathcal{C}}$ with u_w the unique solution of

$$\Delta u_w + k^2 u_w = 0 \quad \text{in } D \quad \text{and} \quad u_w = -w \text{ on } \partial D. \quad (2.15)$$

Note that $H_{\text{inc}}^e(D)$ and \mathcal{G}_k with respect to the scattering poles play the same role that $H_{\text{inc}}(D)$ and \mathcal{W}_k play with respect to the Dirichlet eigenvalues. Thus, we have a new characterization of scattering poles for a Dirichlet obstacle in terms of the kernel of \mathcal{G}_k . To this end, let \mathbb{C}_- denote the complex half-plane of complex numbers with negative imaginary parts. The following equivalence is proven in [23].

Proposition 2.2. $k \in \mathbb{C}_-$ is a scattering pole for a Dirichlet obstacle if and only if \mathcal{G}_k is not injective.

We remark that this definition uses the operator \mathcal{G}_k , hence it still involves the solution of the exterior scattering problem. Again in a similar fashion as for the Dirichlet eigenvalues, we want to use only the scattering operator \mathcal{N}_k in the characterization and computation of the scattering poles. The following theorem states a collection of results proven in [23, Section 2].

Theorem 2.3. Consider $k \in \mathbb{C}_-$. Then

1. The operator $\mathcal{N}_k \varphi = \mathcal{G}_k \text{SL}_{\partial\mathcal{C}}^k(\varphi)$ for all $\varphi \in L^2(\partial\mathcal{C})$.
2. The set $\{\text{SL}_{\partial\mathcal{C}}^k(\varphi); \varphi \in L^2(\partial\mathcal{C})\}$ is dense in $H_{\text{inc}}^e(D)$.
3. The following holds:

- (1) (i) If k is not a scattering pole, then the operators \mathcal{N}_k and \mathcal{G}_k are injective. Furthermore, $\Phi_k(\cdot, z)$ is in the range of \mathcal{G}_k if and only if $z \in \mathbb{R}^m \setminus \overline{D}$.
- (2) (ii) If k is a scattering pole, then $\Phi_k(\cdot, z)$ cannot be in the range of \mathcal{G}_k for a dense set of points z in a ball $\Omega \subset \mathbb{R}^m \setminus \overline{D}$.

The third item of this theorem contains a characterization of the scattering poles in terms of the range of the operator \mathcal{G}_k . It indicates that the equation $\mathcal{G}_k v_z = \Phi_k(\cdot, z)$ has a solution for all points $z \in \mathbb{R}^m \setminus \overline{D}$ if and only if k is not a scattering pole. This is what we would like to exploit numerically. To this end, motivated by item 2 in the theorem, we use a parametrization of the unknown function as $v_z \simeq \text{SL}_{\partial\mathcal{C}}^k(\varphi_z)$ for some $\varphi_z \in L^2(\partial\mathcal{C})$. The advantage of doing so is to transform the equation $\mathcal{G}_k v_z = \Phi_k(\cdot, z)$ into $\mathcal{N}_k \varphi_z \simeq \Phi_k(\cdot, z)$ thanks to item 1 in the theorem, which is numerically cheaper. But the intricate point is then to give a precise definition of the \simeq in the previous identities. The GLSM [22] allows to rigorously define this approximate solution by formulating the equation $\mathcal{N}_k \varphi_z \simeq \Phi_k(\cdot, z)$ as the minimization of a least-square misfit functional with a penalty term that ensures $v_z \simeq \text{SL}_{\partial\mathcal{C}}^k(\varphi_z)$. In the following, we describe this procedure in details. For $\varphi \in L^2(\partial\mathcal{C})$, we set for short notation

$$P_k(\varphi) := \|\text{SL}_{\partial\mathcal{C}}^k(\varphi)\|_{H_{\text{inc}}^e(D)}^2.$$

We then define

$$J_\epsilon(\varphi, \psi) := \epsilon P_k(\varphi) + \|\mathcal{N}_k \varphi(\cdot, z) - \psi\|_{L^2(\partial\mathcal{C})}^2,$$

and set

$$j_\epsilon^z := \inf_{\varphi \in L^2(\partial\mathcal{C})} J_\epsilon(\varphi, \Phi_k(\cdot, z)).$$

We then consider $\varphi_\epsilon^k(\cdot, z)$ to be the minimizing sequence satisfying

$$J_\epsilon(\varphi_\epsilon^k(\cdot, z), \Phi_k(\cdot, z)) \leq j_\epsilon^z + p(\epsilon),$$

where $p(\epsilon)/\epsilon \rightarrow 0$ as $\epsilon \rightarrow 0$. Then, we have the following theorem.

Theorem 2.4. Let $k \in \mathbb{C}_-$. Then for any ball $\Omega \subset \mathbb{R}^m \setminus \overline{D}$

$$\lim_{\epsilon \rightarrow 0} \|\mathcal{N}_k \varphi_\epsilon^k(\cdot, z) - \Phi_k(\cdot, z)\|_{L^2(\partial\mathcal{C})}^2 \rightarrow 0 \quad \text{and} \quad \limsup_{\epsilon \rightarrow 0} P_k(\varphi_\epsilon^k(\cdot, z)) < \infty, \quad (2.16)$$

for a dense set of points $z \in \Omega$ if and only if k is not a scattering pole.

If k is not a scattering pole then the proof of theorem 2.4 follows from the abstract framework of the GLSM provided in [19, Theorem 2.9] with $B = (\text{SL}_{\partial\mathcal{C}}^k)^* \text{SL}_{\partial\mathcal{C}}^k$, along with the injectivity and dense range of \mathcal{N}_k and theorem 2.3(i). In the case when k is a scattering pole, the proof of theorem 2.4 follows the lines of [23, Theorem 2.12].

Theorem 2.4 provides the theoretical foundation of our algorithm for computing the scattering poles from a knowledge of the (computed or measured if possible) interior scattering operator $\mathcal{N}_k : L^2(\partial\mathcal{C}) \rightarrow L^2(\partial\mathcal{C})$. Next, we explain the underlying ideas of the algorithm. To this end, let $\tilde{\mathcal{N}}_k$

be an approximation of \mathcal{N}_k that serves as a regularizer for \mathcal{N}_k^{-1} (see the numerical section below for an example). Based on this theorem, if we set

$$\varphi^k(\cdot, z) := \tilde{\mathcal{N}}_k^{-1} \Phi_k(\cdot, z),$$

where $\tilde{\mathcal{N}}_k^{-1}$ is the pseudo-inverse of $\tilde{\mathcal{N}}_k$, then one expects the quantity

$$\|\mathcal{N}_k \varphi^k(\cdot, z) - \Phi_k(\cdot, z)\|_{L^2(\partial\mathcal{C})}^2 + P_k(\varphi^k(\cdot, z)),$$

to have large values at scattering poles for z in $\Omega \subset \mathbb{R}^m \setminus \overline{D}$. The numerical evaluation of $P_k(\varphi^k(\cdot, z))$ may be time consuming and numerical experiments show that its behaviour with respect to z is similar to the behaviour of the L^2 -norm of the density $\varphi^k(\cdot, z)$. The misfit term $\|\mathcal{N}_k \varphi^k(\cdot, z) - \Phi_k(\cdot, z)\|_{L^2(\partial\mathcal{C})}^2$ is in the majority of the cases small and does not have a significant contribution. Given these observations, we suggest to use the following numerical indicator function to identify the scattering poles:

$$I(k) := \sum_{z \in \mathcal{Z}} \|\tilde{\mathcal{N}}_k^{-1} \Phi_k(\cdot, z)\|_{L^2(\partial\mathcal{C})}^2, \quad (2.17)$$

where \mathcal{Z} is a set of points in $\mathbb{R}^m \setminus \overline{D}$. We expect this indicator function to have larger values at the location of scattering poles.

(a) Numerical algorithm for two-dimensional examples

We provide in this section a possible implementation of the method explained below for two-dimensional problems ($m = 2$). The implementation could be easily adapted in the three-dimensional case by replacing circles by spheres, and the Fourier expansion by the expansion with respect to spherical harmonics. The computational cost does not essentially increase.

The main idea of our implementation method is to take $\partial\mathcal{C}$ to be a circle of radius R_C and translate the coordinate system so that this circle is centred at the origin. In this case, one can express equivalently the operator \mathcal{N}_k using the Fourier transform with respect to the angular coordinate θ and construct a numerical rule to build a low rank $\tilde{\mathcal{N}}_k$ that serves for evaluating (2.17).

A function $\varphi \in L^2(\partial\mathcal{C})$ can be decomposed in the Fourier domain as

$$\varphi(x) = \sum_{n \in \mathbb{Z}} \hat{\varphi}_n e^{-in\theta(x)} \quad \forall x \in \partial\mathcal{C},$$

and we set $\hat{\varphi} = (\hat{\varphi}_n)_{n \in \mathbb{Z}}$, which is an element of $\ell^2(\mathbb{Z})$, the set of square summable sequences. The image of φ by the operator \mathcal{N}_k can be written as

$$\mathcal{N}_k(\varphi)(x) = \sum_{n \in \mathbb{Z}} \hat{\varphi}_n u_n^s(x) \quad x \in \partial\mathcal{C},$$

where we have set

$$u_n^s := \int_{\partial\mathcal{C}} u^s(\cdot, y) e^{-in\theta(y)} ds(y).$$

The functions u_n^s can be computed directly by solving an interior problem. Indeed, thanks to the addition theorem

$$H_0^{(1)}(k|x - y|) = \sum_{m \in \mathbb{Z}} H_n^{(1)}(k|x|) J_n(k|y|) e^{im(\theta(x) - \theta(y))}, \quad |x| > |y|. \quad (2.18)$$

Consequently, for $|y| = R_C$, $x \in \partial D$,

$$- \int_{\theta=0}^{2\pi} \frac{i}{4} H_0^{(1)}(k|x - y|) e^{in\theta(y)} d\theta = \frac{-i\pi}{2} H_n^{(1)}(k|x|) J_n(kR_C) e^{in\theta(x)}.$$

This implies that $u_n^s \in H^1(D)$ is the unique solution to

$$\begin{cases} \Delta u_n^s + k^2 u_n^s = 0 & \text{in } D \\ u_n^s = f_n & \text{on } \partial D, \end{cases} \quad (2.19)$$

where

$$f_n(x) := -\frac{i\pi}{2} H_n^{(1)}(k|x|) J_n(kR_C) e^{in\theta(x)} \quad x \in \partial D.$$

This Dirichlet problem is posed on a bounded domain and can be numerically solved using any standard PDE solver (for instance finite-element methods). For our numerical implementation below, we rather use a boundary integral formulation of this problem based on a single-layer representation of the solution in the form

$$\bar{u}_n^s(x) = \int_{\partial D} \psi(y) H_0^{(1)}(\bar{k}|x - y|) ds(y) \quad \forall x \in D.$$

This leads to a boundary integral equation for ψ of the form

$$\int_{\partial D} \psi(y) H_0^{(1)}(\bar{k}|x - y|) ds(y) = \bar{f}_n(x) \quad \forall x \in \partial D.$$

This equation is approximated using boundary element methods and the resulting system is solved using an LU factorization which has a cost proportional to $N_{\partial D}^3$, where $N_{\partial D}$ is the number of unknowns on the boundary. As a rule of thumb, it is generally admitted that a good approximation is generally obtained for the Helmholtz equation if $N_{\partial D} \sim 2|k||\partial D|$. The important point for our method is that the number of right-hand sides f_n should be much smaller than $N_{\partial D}$, which reduces the numerical cost. This number is related to the way we approximate the operator \mathcal{N}_k , which in turn is related to the size of R_C , which we will explain below in detail.

By introducing the Fourier coefficients of the solution u_n^s

$$\hat{u}_{n,m}^s := \int_{\partial C} u_n^s(x) e^{-im\theta(x)} ds(x),$$

we observe that solving $\mathcal{N}_k \varphi = \psi$ is equivalent in the Fourier domain to solving $\hat{\mathcal{N}}_k \hat{\varphi} = \hat{\psi}$, where the operator $\hat{\mathcal{N}}_k : \ell^2(\mathbb{Z}) \rightarrow \ell^2(\mathbb{Z})$ is defined by

$$(\hat{\mathcal{N}}_k \hat{\varphi})_m := \sum_{n \in \mathbb{Z}} \hat{u}_{n,m}^s \hat{\varphi}_n.$$

As a numerical approximation of this operator, we shall use the operator $\hat{\mathcal{N}}_k^N : \mathbb{C}^{2N+1} \rightarrow \mathbb{C}^{2N+1}$ defined by

$$(\hat{\mathcal{N}}_k^N \hat{\varphi})_m := \sum_{n=-N}^{n=N} \hat{u}_{n,m}^s \hat{\varphi}_n, \quad -N \leq m \leq N,$$

where $N > 0$ is some truncation parameter that will be chosen later.

Let us denote by $(\hat{\Phi}_k(z))_{n \in \mathbb{Z}} \in \ell^2(\mathbb{Z})$ the Fourier transform of $\Phi_k(\cdot, z)$. The addition formula shows that

$$(\hat{\Phi}_k(z))_n = \frac{i\pi}{2} H_n^{(1)}(k|z|) J_n(kR_C) e^{in\theta(z)}.$$

Let $\hat{\Phi}_k^N(z) \in \mathbb{C}^{2N+1}$ be the vector formed by $(\hat{\Phi}_k(z))_n$ with $n = -N, \dots, N$. Equivalently to (2.17), we shall use as indicator function for scattering poles, the function

$$\hat{I}(k) := \sum_{z \in \mathcal{Z}} \|(\hat{\mathcal{N}}_k^N)^{-1} \hat{\Phi}_k^N(z)\|_{\mathbb{C}^{2N+1}}^2. \quad (2.20)$$

Note that (similarly to \mathcal{N}_k) the operator $\hat{\mathcal{N}}_k$ is a compact operator, thus the inverse operator is unbounded. The truncation N serves as a regularization parameter, it is a trade-off between the approximation error and ill-conditioning. To mitigate the latter, N cannot be chosen too large in order to keep the conditioning number of the matrix $\hat{\mathcal{N}}_k^N$ small enough by ignoring small singular values. Note that in practice the truncation parameter N would depend on R_C and k

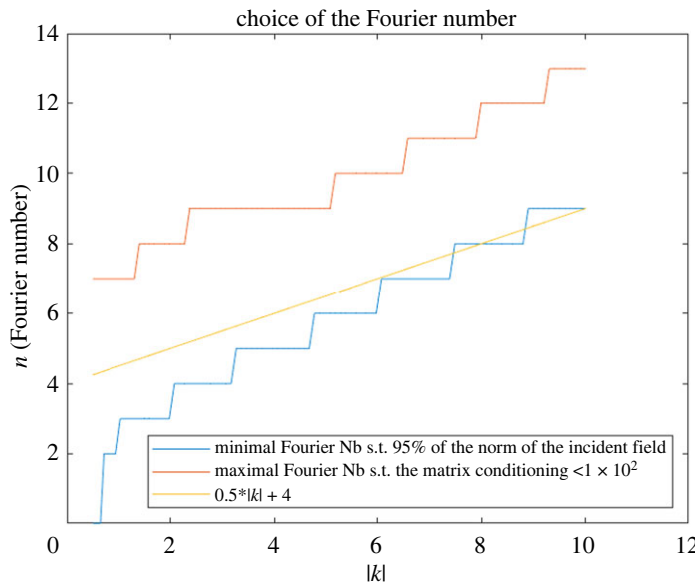


Figure 1. Choice of the cut-off value for Fourier coefficients.

(see discussion in §4, figure 1 where a rule of thumb $N \sim |k|R_C + 4$ is observed) and this number is expected to be small compared with $N_{\partial D}$. The latter is ensured by controlling the size of R_C . Reducing R_C (i.e. the size of the inner circle) reduces the numerical cost of the method but at the expense of less accuracy and vice versa. Indeed, one can imagine a greedy procedure where the size of R_C is gradually increased as the location of the scattering poles improves. This aspect is not included in our numerical implementation below. The evaluation of $\hat{I}(k)$ is done in our implementation by using a singular value decomposition of $\hat{\mathcal{N}}_k^N$, for which the cost is $O(N^3)$.

(i) Analytic expression in the case of circular domain

In the case of a circular domain, it is possible to have an analytic expression of the operator $\hat{\mathcal{N}}_k$ and therefore an analytic expression of $\hat{I}(k)$. Assume that the domain D is the disc of radius R_D . In this case, the scattering poles are formed by the zeros of $k \mapsto H_n^{(1)}(kR_D)$. For $k \in \mathbb{C}_-$, the scattered field u_n^s solution of (2.19) is then given by

$$u_n^s(x) = \frac{-i\pi}{2} \frac{H_n^{(1)}(kR_D)J_n(kR_C)}{J_n(kR_D)} J_n(k|x|) e^{in\theta(x)}.$$

This leads to

$$\hat{u}_{n,n}^s = -i\pi^2 R_C \frac{H_n^{(1)}(kR_D)J_n(kR_C)^2}{J_n(kR_D)} \quad \text{and} \quad \hat{u}_{n,m}^s = 0 \text{ if } n \neq m,$$

which indicates that the operator $\hat{\mathcal{N}}_k^N$ is diagonal and invertible for all $k \in \mathbb{C}_-$ outside the scattering poles. One then obtains

$$\hat{I}(k) := \frac{1}{2\pi R_C} \sum_{z \in \mathcal{Z}} \sum_{n=-N}^{n=N} \left| \frac{J_n(kR_D)H_n^{(1)}(k|z|)}{H_n^{(1)}(kR_D)J_n(kR_C)} \right|^2.$$

This expression clearly shows that if we choose $|z| > R_D$ to form a dense set in an interval, $\hat{I}(k) \rightarrow \infty$ as k approaches any scattering poles that are zeros of $H_n^{(1)}(kR_D)$ for $-N \leq n \leq N$.

3. Extension to the scattering problem for an impedance obstacle

The algorithm described above and the related theory can be naturally extended to other boundary conditions. The advantage of our computational method for the scattering poles is that once the interior scattering operator $\mathcal{N}_k : L^2(\partial\mathcal{C}) \rightarrow L^2(\partial\mathcal{C})$ corresponding to that scattering problem is available then in principle the algorithm is implemented in the same way without making use of the physical properties of the scatterer. We describe this extension in the case of the scattering problem for an obstacle with impedance boundary conditions. Under the same assumption for D the scattering problem now reads

$$\left. \begin{aligned} \Delta u^s + k^2 u^s &= 0 && \text{in } \mathbb{R}^m \setminus \bar{D} \\ \frac{\partial u^s}{\partial \nu} + ik\eta u^s &= -\left(\frac{\partial v}{\partial \nu} + ik\eta v\right) && \text{on } \partial D \\ \lim_{r \rightarrow \infty} r^{(m-1)2} \left(\frac{\partial u^s}{\partial r} - iku^s\right) &= 0, \end{aligned} \right\} \quad (3.1)$$

where $\eta \in L^\infty(\partial D)$ such that $\Re(\eta)(x) \geq 0$ for almost all $x \in \partial D$. This problem is well-posed for $k \in \mathbb{C}$ with $\Im(k) \geq 0$. Note that our approach can be generalized verbatim to k dependent η which model dispersive thin layer coating D . More specifically in this case one assumes that $\eta = \eta(k)$ depends analytically on k and is such that $\Im(\eta(k)) < 0$ if $k \in \mathbb{C}_-$. However, for the purpose of presentation here, we assume that η is independent of k . Under these assumptions, we can define the scattering poles for an impedance obstacle. The above scattering problem can be equivalently written as given $f \in H^{-1/2}(\partial D)$ find $w \in H^1_{\text{loc}}(\mathbb{R}^m \setminus D)$ such that

$$\left\{ \begin{aligned} \Delta w + k^2 w &= 0 && \text{in } \mathbb{R}^m \setminus \bar{D} \\ \frac{\partial w}{\partial \nu} + ik\eta w &= f && \text{on } \partial D \\ w &= \text{SL}_{\partial D}^k \left(\frac{\partial w}{\partial \nu} \right) - \text{DL}_{\partial D}^k(w) && \text{in } \mathbb{R}^m \setminus \bar{D}. \end{aligned} \right. \quad (3.2)$$

Definition 3.1. $k \in \mathbb{C}$ is a scattering pole of the scattering problem for D with impedance boundary conditions if the homogeneous problem (3.2), i.e. with $f = 0$, has a non-trivial solution.

Under the above assumptions on η , it is known that these scattering poles lie in the complex lower half-plane $\mathbb{C}_- := \{z \in \mathbb{C}, \Im(z) < 0\}$ and form a discrete set without accumulation points [26]. The corresponding interior scattering problem is now formulated as: for a point $z \in D$, $u^s(\cdot, z) \in H^1(D)$ is the unique solution of

$$\left\{ \begin{aligned} \Delta u^s(\cdot, z) + k^2 u^s(\cdot, z) &= 0 && \text{in } D \\ \frac{\partial u^s(\cdot, z)}{\partial \nu} + ik\eta u^s(\cdot, z) &= -\left(\frac{\partial \Phi_k(\cdot, z)}{\partial \nu} + i\eta \Phi_k(\cdot, z)\right) && \text{on } \partial D. \end{aligned} \right. \quad (3.3)$$

Since we are interested in the scattering poles, we restrict $k \in \mathbb{C}_-$, and this problem has a unique solution since the impedance eigenvalues have positive imaginary part. One then defines the operator \mathcal{N}_k the same way as (2.10) where now $u^s(x, z)$ is given by (3.3).

Theorem 3.2. *Assume $k \in \mathbb{C}_-$ is not a scattering pole. Then the operator $\mathcal{N}_k : L^2(\partial\mathcal{C}) \rightarrow L^2(\partial\mathcal{C})$ is injective.*

Proof. Let $g \in L^2(\partial\mathcal{C})$ be such that $\mathcal{N}_k(g) = 0$ on $\partial\mathcal{C}$. u_g^s solves the Helmholtz equation in $D \supset \mathcal{C}$ and $u_g^s|_{\partial\mathcal{C}} = 0$, and since k^2 is not a Dirichlet eigenvalue in \mathcal{C} , $u_g^s = 0$ in \mathcal{C} . By a unique continuation $u_g^s = 0$ in D and hence $\frac{\partial u_g^s}{\partial \nu} + ik\eta u_g^s = 0$ on ∂D . By linearity and superposition $-\left(\frac{\partial u_g^s}{\partial \nu} + ik\eta u_g^s\right) = \text{SL}_{\partial\mathcal{C}}(g) + ik\eta \text{SL}_{\partial\mathcal{C}}(g) = 0$ on ∂D . Since $\text{SL}_{\partial\mathcal{C}}(g)$ solves (3.2) with $f = 0$ and since k is not a scattering pole of the impedance problem, $\text{SL}_{\partial\mathcal{C}}(g) = 0$ in $\mathbb{R}^m \setminus \bar{D}$, and by unique continuation, in $\mathbb{R}^3 \setminus \mathcal{C}$. In addition, we also have $\text{SL}_{\partial\mathcal{C}}(g) = 0$ in \mathcal{C} . Finally, using the jump relation on $\partial\mathcal{C}$ for the normal derivative of the single-layer potential [25], we obtain $g = 0$. ■

By obvious modifications of the proof of [23, Lemma 2.5], we can prove the following lemma:

Lemma 3.3. *The operator \mathcal{N}_k is symmetric, that is its transpose operator $\mathcal{N}_k^T : L^2(\partial\mathcal{C}) \rightarrow L^2(\partial\mathcal{C})$ verifies $\mathcal{N}_k^T(g) = \mathcal{N}_k(g)$, where \mathcal{N}_k^T is defined by*

$$\int_{\partial\mathcal{C}} \mathcal{N}_k(g)(x)f(x) \, ds(x) = \int_{\partial\mathcal{C}} g(x)\mathcal{N}_k^T(f)(x) \, ds(x) \quad \forall f, g \in L^2(\partial\mathcal{C}).$$

Combining theorem 3.4 and lemma 3.3, we conclude that

Theorem 3.4. *Assume $k \in \mathbb{C}_-$ is not a scattering pole. Then the operator $\mathcal{N}_k : L^2(\partial\mathcal{C}) \rightarrow L^2(\partial\mathcal{C})$ has dense range.*

In the impedance case, the operator $\mathcal{G}_k : H_{\text{inc}}^e(D) \rightarrow L^2(\partial\mathcal{C})$ maps $w \mapsto u_w|_{\partial\mathcal{C}}$ with u_w the unique solution of

$$\Delta u_w + k^2 u_w = 0 \quad \text{in } D \quad \text{and} \quad \frac{\partial u_w}{\partial \nu} + ik\eta u_w = -\left(\frac{\partial w}{\partial \nu} + ik\eta w\right) \quad \text{on } \partial D. \quad (3.4)$$

We next prove an equivalent definition of the scattering poles with definition 3.1.

Proposition 3.5. *$k \in \mathbb{C}_-$ is a scattering pole for an impedance obstacle if and only if \mathcal{G}_k is not injective.*

Proof of the equivalence of definitions 3.1 and 3.5.

- (i) Let us suppose k is a scattering pole for the impedance problem in D and write $w_0 \in H_{\text{inc}}^e(D)$ its associated eigenfunction, where $H_{\text{inc}}^e(D)$ given by (2.13). Then $\frac{\partial w_0}{\partial \nu} + ik\eta w_0 = 0$ on ∂D , therefore as k is not an eigenvalue of the impedance problem in D , $u_{w_0} = 0$ in D and therefore $\mathcal{G}_k(w_0) = 0$.
- (ii) Conversely, let us suppose there exists a non-trivial $w_0 \in H_{\text{inc}}^e(D)$ such that $\mathcal{G}_k(w_0) = 0$. Then $u_{w_0} = 0$ on $\partial\mathcal{C}$ and as k is not a Dirichlet eigenvalue in \mathcal{C} , $u_{w_0} = 0$ in \mathcal{C} and by unique continuation, in D . By uniqueness of the impedance problem in D , $\frac{\partial u_{w_0}}{\partial \nu} + ik\eta u_{w_0} = 0$ on ∂D , and therefore $\frac{\partial w_0}{\partial \nu} + ik\eta w_0 = 0$ on ∂D . That is w_0 is an eigenfunction of the impedance boundary problem, i.e. k is a scattering pole of the impedance problem.

■

Lemma 3.6. *Assume $k \in \mathbb{C}_-$ is not a scattering pole of the impedance problem in D , and let $z \in \mathbb{R}^m \setminus \overline{\mathcal{C}}$. Then $\Phi_k(\cdot, z)$ is in the range of \mathcal{G}_k if and only if $z \in \mathbb{R}^m \setminus \overline{D}$.*

Proof.

- (i) If $z \in \mathbb{R}^m \setminus \overline{D}$, then we find $w \in H_{\text{inc}}^e(D)$ to be the unique solution of the exterior impedance problem (3.2) with the right-hand side $f = \frac{\partial \Phi_k(\cdot, z)}{\partial \nu} + ik\eta \Phi_k(\cdot, z)$ on ∂D . By uniqueness of the impedance problem in D , we immediately have $\mathcal{G}_k(w) = \Phi_k(\cdot, z)|_{\mathcal{C}}$.
- (ii) Conversely, assume to the contrary that for $z \in D \setminus \overline{\mathcal{C}}$, there exists $w \in H_{\text{inc}}^e(D)$ such that $\mathcal{G}_k(w) = \Phi(\cdot, z)$. This means that there exists u_w satisfying (3.4) with $u_w = \Phi_k(\cdot, z)$ on $\partial\mathcal{C}$. Since both u_w and $\Phi(\cdot, z)$ satisfy the Helmholtz equation in \mathcal{C} then by the uniqueness of the Dirichlet problem $u_w = \Phi_k(\cdot, z)$ in \mathcal{C} and hence in D by unique continuation. This is a contradiction since $u_w \in H^1(D \setminus \overline{\mathcal{C}})$ and $\Phi_k(\cdot, z) \notin H^1(D \setminus \overline{\mathcal{C}})$.

■

Lemma 3.7. *Assume $k \in \mathbb{C}_-$ is a scattering pole of the impedance problem in D . Then $\Phi_k(\cdot, z)$ cannot be in the range of \mathcal{G}_k for a dense set of points z in a ball $\Omega \subset \mathbb{R}^m \setminus \overline{D}$.*

Proof. Assume that $k \in \mathbb{C}_-$ is a scattering pole and let w_0 be the solution of (3.2) with $f = 0$. Assume to the contrary that for a dense set of points $z \in \Omega$ we have that $\mathcal{G}_k(w_z) = \Phi(\cdot, z)$ with $w_z \in H_{\text{inc}}^e(D)$. Thus, we have that there exists the corresponding $u_z \in H^1(D)$ satisfying (3.4) and $u_z|_{\partial\mathcal{C}} = \Phi_z(\cdot, z)$. We deduce by uniqueness of the Dirichlet problem inside \mathcal{C} that $u_z = \Phi_k(\cdot, z)$ in \mathcal{C}

and by unique continuation in D . By uniqueness of the impedance boundary problem in D , we have $\frac{\partial u_z}{\partial \nu} + ik\eta u_z = \frac{\partial \Phi_k(\cdot, z)}{\partial \nu} + ik\eta \Phi_k(\cdot, z)$ on ∂D , that is $\frac{\partial w_z}{\partial \nu} + ik\eta w_z = \frac{\partial \Phi_k(\cdot, z)}{\partial \nu} + ik\eta \Phi_k(\cdot, z)$ on ∂D .

For a generic $m - 1$ dimensional closed Lipschitz manifold without boundary $\partial\mathcal{O}$ introduce the boundary integral operators obtained from (2.6) and (2.7) and their derivative by approaching the boundary $\partial\mathcal{O}$

$$\mathcal{S}_{\partial\mathcal{O}}^k : H^{-1/2}(\partial\mathcal{O}) \rightarrow H^{1/2}(\partial\mathcal{O}) \quad \psi \mapsto \int_{\partial\mathcal{O}} \psi(y) \Phi_k(\cdot, y) \, ds(y),$$

$$\mathcal{K}_{\partial\mathcal{O}}^k : H^{1/2}(\partial\mathcal{O}) \rightarrow H^{1/2}(\partial\mathcal{O}) \quad \psi \mapsto \int_{\partial\mathcal{O}} \psi(y) \frac{\partial \Phi_k(\cdot, y)}{\partial \nu_y} \, ds(y),$$

$$\tilde{\mathcal{K}}_{\partial\mathcal{O}}^k : H^{-1/2}(\partial\mathcal{O}) \rightarrow H^{-1/2}(\partial\mathcal{O}) \quad \psi \mapsto \int_{\partial\mathcal{O}} \psi(y) \frac{\partial \Phi_k(\cdot, y)}{\partial \nu_v} \, ds(y)$$

and

$$\mathcal{L}_{\partial\mathcal{O}}^k : H^{1/2}(\partial\mathcal{O}) \rightarrow H^{-1/2}(\partial\mathcal{O}) \quad \psi \mapsto \frac{\partial}{\partial \nu} \int_{\partial\mathcal{O}} \psi(y) \frac{\partial \Phi_k(\cdot, y)}{\partial \nu_y} \, ds(y).$$

Applying the impedance boundary condition on Green's representation formula for w_0 approaching ∂D from the outside, we have

$$\left(\tilde{\mathcal{K}}_{\partial D}^k - \frac{1}{2} + ik\eta \mathcal{S}_{\partial D}^k \right) \frac{\partial w_0}{\partial \nu} - \left(\mathcal{L}_{\partial D}^k + ik\eta \mathcal{K}_{\partial D}^k + \frac{ik\eta}{2} \right) w_0 = 0,$$

and using $\frac{\partial w_0}{\partial \nu} = -ik\eta w_0$ yields

$$(ik\eta \tilde{\mathcal{K}}_{\partial D}^k + (ik\eta)^2 \mathcal{S}_{\partial D}^k + \mathcal{L}_{\partial D}^k + ik\eta \mathcal{K}_{\partial D}^k) w_0 = 0. \quad (3.5)$$

In a similar way, we have the impedance boundary condition of w_z by approaching ∂D from outside in Green's representation formula

$$\frac{\partial w_z}{\partial \nu} + ik\eta w_z = - \left(\tilde{\mathcal{K}}_{\partial D}^k - \frac{1}{2} + ik\eta \mathcal{S}_{\partial D}^k \right) \frac{\partial w_z}{\partial \nu} + \left(\mathcal{L}_{\partial D}^k + ik\eta \mathcal{K}_{\partial D}^k + \frac{ik\eta}{2} \right) w_z,$$

which we can write as

$$\frac{\partial w_z}{\partial \nu} + ik\eta w_z = -2(\tilde{\mathcal{K}}_{\partial D}^k + ik\eta \mathcal{S}_{\partial D}^k) \frac{\partial w_z}{\partial \nu} + 2(\mathcal{L}_{\partial D}^k + ik\eta \mathcal{K}_{\partial D}^k) w_z. \quad (3.6)$$

Taking now the trace of the representation formula u_z and its normal derivative on ∂D from inside yields

$$\frac{\partial u_z}{\partial \nu} + ik\eta u_z = \left(\tilde{\mathcal{K}}_{\partial D}^k + \frac{1}{2} + ik\eta \mathcal{S}_{\partial D}^k \right) \frac{\partial u_z}{\partial \nu} - \left(\mathcal{L}_{\partial D}^k + ik\eta \mathcal{K}_{\partial D}^k - \frac{ik\eta}{2} \right),$$

or equivalently

$$\frac{\partial u_z}{\partial \nu} + ik\eta u_z = 2(\tilde{\mathcal{K}}_{\partial D}^k + ik\eta \mathcal{S}_{\partial D}^k) \frac{\partial u_z}{\partial \nu} - 2(\mathcal{L}_{\partial D}^k + ik\eta \mathcal{K}_{\partial D}^k) u_z. \quad (3.7)$$

Next, we multiply (3.7) by w_0 and integrate over ∂D . Using $\frac{\partial u_z}{\partial \nu} = -ik\eta u_z + \frac{\partial w_z}{\partial \nu} + ik\eta w_z$, we obtain that

$$\int_{\partial D} \frac{\partial \Phi_k(\cdot, z)}{\partial \nu} w_0 + ik\eta \Phi_k(\cdot, z) w_0 \, ds = \int_{\partial D} \frac{\partial u_z}{\partial \nu} + ik\eta u_z w_0 \, ds$$

$$= \int_{\partial D} 2(\tilde{\mathcal{K}}_{\partial D}^k + ik\eta \mathcal{S}_{\partial D}^k) \frac{\partial u_z}{\partial \nu} w_0 - 2(\mathcal{L}_{\partial D}^k + ik\eta \mathcal{K}_{\partial D}^k) u_z w_0 \, ds$$

$$= \int_{\partial D} 2(\tilde{\mathcal{K}}_{\partial D}^k + ik\eta \mathcal{S}_{\partial D}^k) \left(\frac{\partial w_z}{\partial \nu} + ik\eta w_z \right) w_0 \, ds$$

$$- \int_{\partial D} 2(ik\eta \tilde{\mathcal{K}}_{\partial D}^k + (ik\eta)^2 \mathcal{S}_{\partial D}^k + \mathcal{L}_{\partial D}^k + ik\eta \mathcal{K}_{\partial D}^k) u_z w_0 \, ds.$$

Thanks to the identities $\mathcal{K}_{\partial D}^k \top = \tilde{\mathcal{K}}_{\partial D}^k$, $\mathcal{L}_{\partial D}^k \top = \mathcal{L}_{\partial D}^k$ and $\mathcal{S}_{\partial D}^k \top = \mathcal{S}_{\partial D}^k$ [25] and the relation (3.5), the second integral is zero. We now use the identity (3.6) to replace $2(\tilde{\mathcal{K}}_{\partial D}^k + ik\eta\mathcal{S}_{\partial D}^k)\frac{\partial w_z}{\partial v}$ in the first integral, which gives

$$\begin{aligned} \int_{\partial D} \frac{\partial \Phi_k(\cdot, z)}{\partial v} w_0 + ik\eta \Phi_k(\cdot, z) w_0 \, ds &= - \int_{\partial D} \left(\frac{\partial w_z}{\partial v} + ik\eta w_z \right) w_0 \, ds \\ &\quad + 2 \int_{\partial D} (\mathcal{L}_{\partial D}^k + ik\eta \mathcal{K}_{\partial D}^k + ik\eta \tilde{\mathcal{K}}_{\partial D}^k + (ik\eta)^2 \mathcal{S}_{\partial D}^k) w_z w_0 \, ds. \end{aligned}$$

Knowing $\frac{\partial w_z}{\partial v} + ik\eta w_z = \frac{\partial \Phi_k(\cdot, z)}{\partial v} + ik\eta \Phi_k(\cdot, z)$ and using again (3.5), we can conclude that

$$u(z) := \int_{\partial D} \frac{\partial \Phi_k(\cdot, z)}{\partial v} w_0 + ik\eta \Phi_k(\cdot, z) w_0 \, ds = \text{DL}_{\partial D}^k(w_0)(z) - \text{SL}_{\partial D}^k\left(\frac{\partial w_0}{\partial v}\right)(z) = 0$$

for a dense set of points z in Ω , where we use that $ik\eta w_0 = -\frac{\partial w_0}{\partial v}$. Since $u(z)$ is a solution to the Helmholtz equation in $\mathbb{R}^m \setminus \overline{D}$ hence analytic, we conclude that $u(z) = 0$ in $\mathbb{R}^m \setminus \overline{D}$. On the other hand, $u(z)$ as a solution of Helmholtz equation inside D . Letting z approach the boundary from both sides, using the jump relations of single and double potentials, and knowing that $u^+|_{\partial D} = \frac{\partial u^+}{\partial v}|_{\partial D} = 0$ (traces from outside D) give

$$\frac{\partial u^-}{\partial v} + ik\eta u^- = \frac{\partial w_0}{\partial v} + ik\eta w_0 = 0. \quad (3.8)$$

Therefore, by uniqueness of the impedance problem inside D , we conclude $u = 0$ in D . Using the jump relation of u over ∂D , we have $w_0|_{\partial D} = (\partial w_0/\partial v)|_{\partial D} = 0$. By Holmgren's theorem $w_0 = 0$ in $\mathbb{R}^m \setminus \overline{D}$, which is a contradiction. This proves the lemma. ■

Obviously, we have that $\mathcal{N}_k \varphi = \mathcal{G}_k \text{SL}_{\partial C}^k(\varphi)$ for all $\varphi \in L^2(\partial C)$ and that $\{\text{SL}_{\partial C}^k(\varphi); \varphi \in L^2(\partial C)\}$ is dense in $H_{\text{inc}}^e(D)$. Thus, the above discussion provides all the ingredients to prove theorem 2.4, which is the theoretical basis of our computational algorithm.

(a) Numerical algorithm for two-dimensional examples

In a similar way as for the Dirichlet problem in §2a, for the numerical implementation of the algorithm in the two-dimensional case, we can obtain an explicit expression of the operator $\hat{\mathcal{N}}_k$ in the Fourier domain. For the impedance problem, the functions u_n^s are now defined as the unique solution in $H^1(D)$ of

$$\begin{cases} \Delta u_n^s + k^2 u_n^s = 0 & \text{in } D \\ \frac{\partial u_n^s}{\partial v} + i\eta(k)u_n^s = f_n & \text{on } \partial D, \end{cases} \quad (3.9)$$

where

$$f_n(x) := \left(\frac{\partial}{\partial v} + ik\eta \right) \left(\frac{-i\pi}{2} H_n^{(1)}(k|x|) J_n(kR_C) e^{in\theta(x)} \right) \quad x \in \partial D.$$

Using the formula for Bessel and Hankel functions

$$\mathcal{X}'_n(x) = -\mathcal{X}_{n+1}(x) + \frac{n}{x} \mathcal{X}_n(x), \quad (3.10)$$

for $\mathcal{X}_n = H_n^{(1)}$ or J_n , we end up with

$$f_n(x) = \frac{i\pi}{2} J_n(kR_C) e^{in\theta(x)} \left[(-kH_{n+1}^{(1)}(k|x|) + \frac{n}{|x|} H_n^{(1)}(k|x|)) \frac{x \cdot v}{|x|} + i\eta(k) H_n^{(1)}(k|x|) \right].$$

The rest of the implementation works in the same way as in §2a.

(i) Analytic expression in the case of a circular domain

Assume that the domain D is the disc of radius R_D centred at the origin and $\eta := \eta(k)$ does not depend on the angular variable. Then, the scattering poles are the zeros of the functions

$$f_n(k) := -kH_{n+1}^{(1)}(kR_D) + \left(\frac{n}{R_D} + i\eta(k)\right)H_n^{(1)}(kR_D). \quad (3.11)$$

One can solve explicitly for u_n^s and get

$$u_n^s(x) = \frac{-i\pi}{2} J_n(kR_C) \frac{\left[-kH_{n+1}^{(1)}(kR_D) + \left(\frac{n}{R_D} + i\eta(k)\right)H_n^{(1)}(kR_D)\right]}{\left[-kJ_{n+1}(kR_D) + \left(\frac{n}{R_D} + i\eta(k)\right)J_n(kR_D)\right]} J_n(k|x|) e^{in\theta(x)}.$$

This again leads to a diagonal operator $\hat{\mathcal{N}}_k$ with diagonal terms given by

$$\hat{u}_{n,n}^s = -i\pi^2 R_C J_n(kR_C)^2 \frac{\left[-kH_{n+1}^{(1)}(kR_D) + \left(\frac{n}{R_D} + i\eta(k)\right)H_n^{(1)}(kR_D)\right]}{\left[-kJ_{n+1}(kR_D) + \left(\frac{n}{R_D} + i\eta(k)\right)J_n(kR_D)\right]}.$$

Consequently, the truncated indicator function takes the expression

$$\hat{I}(k) = \frac{1}{2\pi R_C} \sum_{z \in \mathcal{Z}} \sum_{n=-N}^{n=N} \left| \frac{H_n^{(1)}(k|z|)}{J_n(kR_C)} \frac{\left[-kJ_{n+1}(kR) + \left(\frac{n}{R} + i\eta(k)\right)J_n(kR)\right]}{\left[-kH_{n+1}^{(1)}(kR) + \left(\frac{n}{R} + i\eta(k)\right)H_n^{(1)}(kR)\right]} \right|^2.$$

We again observe that this indicator function goes to ∞ as k approaches a scattering poles if the points z are chosen such that they are not zeros of $H_n^{(1)}(k|z|)$.

4. Numerical validation

To build the matrix $\hat{\mathcal{N}}_k$, we use Gypsilab [27], an open MATLAB toolbox, which enables us to solve our boundary value problems (2.19) (and (3.9) in the case of impedance boundary conditions) using boundary integral techniques. As indicated earlier, any other numerical solver could have been used for this step.

A key parameter in our method is the choice of N , the number of Fourier parameter used in truncating the operator $\hat{\mathcal{N}}_k$. This number is tuned in order to control the conditioning of the matrix operator $\hat{\mathcal{N}}_k^N$. Indeed, in the case of a circle, one can see from the analytical expressions derived above that the conditioning grows exponentially with respect to N . On the other hand, a number of Fourier coefficients that is too small will lower the precision as it would not allow to reach scattering poles that are the zeros of Hankel functions with order greater than N . This is specific to the circles. For general domains, we may rephrase this requirement as a precision constraint, meaning that $\hat{\mathcal{N}}_k^N$ should be a sufficiently accurate approximation of $\hat{\mathcal{N}}_k$. It is also related to the fact that the incident field $\Phi(\cdot, z)$ for $z \in \mathcal{C}$ should be accurately approximated on ∂D by its truncated Fourier series.

We first consider the case where D is the unit disc and ∂C be the circle of radius $1/2$. We plot in figure 1, the number of Fourier coefficients for different values of $k = \Re(k) - 0.5i$, with $\Re(k) \in [0; 20]$ for the case of Dirichlet boundary conditions. The number of Fourier coefficients N is chosen between the maximum value such that the condition number of $\hat{\mathcal{N}}_k^N$ stays below 10^2 , and the minimum value to reach 95% of the norm of the incident field.

As a rule of thumb, choosing $N \sim |k|R_C + 4$, seems to provide a good balance. This has been confirmed by many other experiments not reported here. This choice is the one adopted in the following experiments.

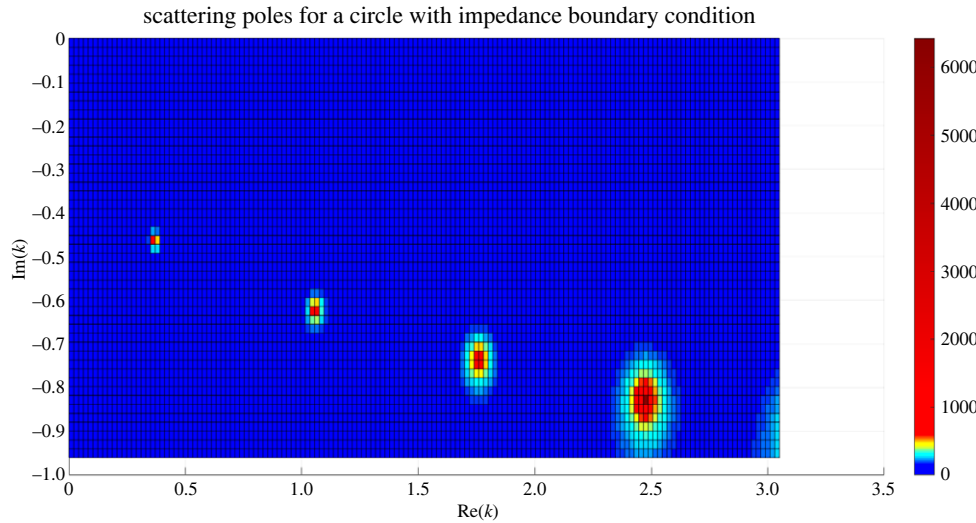


Figure 2. The indicator function $\hat{\ell}(k)$ for a circle of radius 1.3 and an impedance $\eta(k) = k/10$.

(a) Validation in the case of a disc

It is possible to numerically determine the scattering poles as the zeros of the functions f_n given by (3.11). We exploit the Cauchy integral to compute these zeros, using the identity

$$\frac{1}{2i\pi} \int_{\gamma} k^{\ell} \frac{f'_n(k)}{f_n(k)} dk = \sum_{i=1}^M m_i k_i^{\ell},$$

where k_i , $i = 1, \dots, M$, are the zeros inside the direct contour γ and m_i are their order. Using $\ell = 1$, this allows an accurate evaluation of scattering poles that have simple multiplicities by choosing the contour γ to be sufficiently small so that it contains only one pole. The number of poles lying inside γ can be determined using $\ell = 0$. For f_n given by (3.11), the derivative is given by

$$\frac{df}{dk} = kRH_{n+2}(kR) - (2(n+1) - R\eta(k))H_{n+1}(kR) + \left(i\eta'(k) + \frac{n}{k}i\eta + \frac{n^2}{kR} \right) H_n(kR).$$

We take a circle of radius $R = 1.3$ and an impedance function $\eta(k) = k/10$. Thanks to the Cauchy integral, we find the poles of f

$$\begin{cases} k_1 = 0.3593 - 0.4712i & \text{for } n = 1 \\ k_2 = 1.0490 - 0.6304i & \text{for } n = 2 \\ k_3 = 1.7514 - 0.7435i & \text{for } n = 3 \\ k_4 = 2.4627 - 0.8346i & \text{for } n = 4. \end{cases}$$

Searching in the area $[0; 3] \times [-1; 0]$, we compute $\hat{\ell}(k)$ for values of k in a uniform grid with a step size 2×10^{-2} . Figure 2 displays the obtained indicator function where we clearly see the peaks at the location of the scattering poles. The coordinates of the peaks (with the used mesh step) give the following approximations for these scattering poles:

$$\begin{cases} k_1^{\text{res}} = 0.3503 - 0.4704i \\ k_2^{\text{res}} = 1.0554 - 0.6336i \\ k_3^{\text{res}} = 1.7606 - 0.7356i \\ k_4^{\text{res}} = 2.4657 - 0.8376i. \end{cases}$$

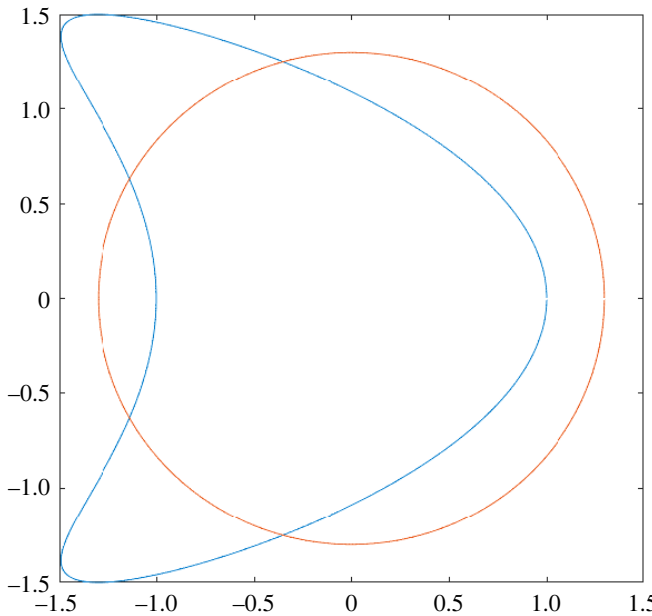


Figure 3. Geometry of a kite compared with the circle of radius 1.3.

(b) The case of a kite

We consider a different shape, a kite which is a deformation of a circle that has the geometry described in [figure 3](#). The equation of the kite is given by

$$\mathcal{K}(\theta) = (\cos(\theta) + 0.65 \cos(2\theta) - 0.65, 1.5 \sin(\theta)), \quad \theta \in [0; 2\pi].$$

Searching in the same area as in the previous example, we get four peaks corresponding to four scattering poles ([figure 4](#))

$$\begin{cases} k_1^{\text{res}} = 0.3707 - 0.4908i \\ k_2^{\text{res}} = 1.1798 - 0.6336i \\ k_3^{\text{res}} = 2.0464 - 0.8176i \\ k_4^{\text{res}} = 2.9292 - 0.9000i. \end{cases}$$

Seeing the kite as a deformation of the circle, we can compare the values of their poles. They count the same number of poles, so we can pair them. The greater the distance to the origin, the less similar the poles seem to be ([figure 5](#)).

(c) The influence of the impedance parameter

We can see that for $\eta = 0$, the problem corresponds to the Neumann boundary value problem, and for $\eta \rightarrow \infty$ it becomes the Dirichlet boundary value problem. It is interesting to observe the behaviour of a particular scattering pole when the boundary condition on the scatterer changes from Dirichlet to Neumann via an impedance boundary condition with a constant impedance parameter η varying in $[0, \infty)$. The scattering pole is continuous with respect to η , as we can see in [figure 6](#) (where the parameter η is varied from 0 to 50 taking 60 equally distributed values). For each fixed such η , the coordinates of the scattering pole corresponding to the impedance boundary condition $(\partial/\partial\nu) + ik\eta$ are computed based on the numerical scheme described above.

We observe that the continuous dependence of the scattering pole with respect to η takes a 'stair shape'. If the problem is close to a Dirichlet problem (η large), the real part of the Dirichlet pole is a good approximation for the real part of the impedance pole. And if the problem is close to

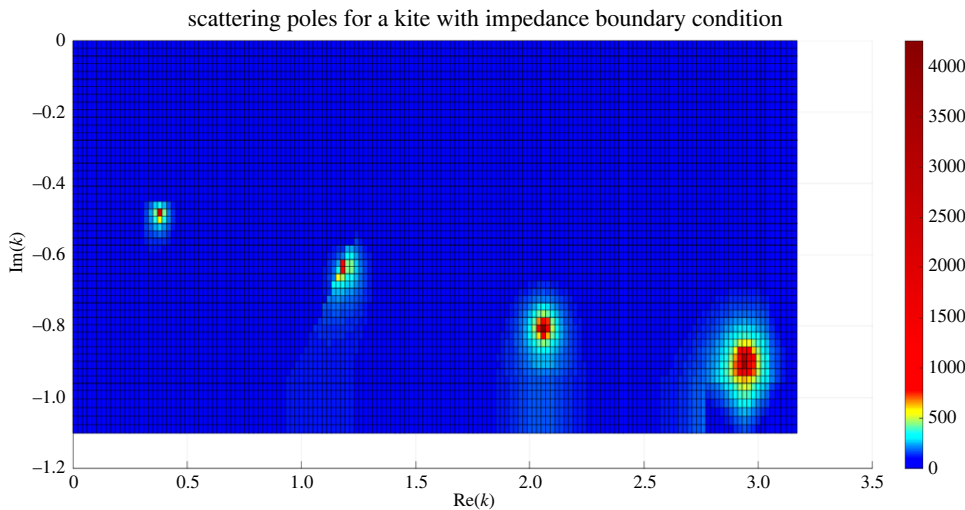


Figure 4. The indicator function $\hat{\iota}(k)$ for the kite depicted in figure 3 and an impedance $\eta(k) = k/10$.

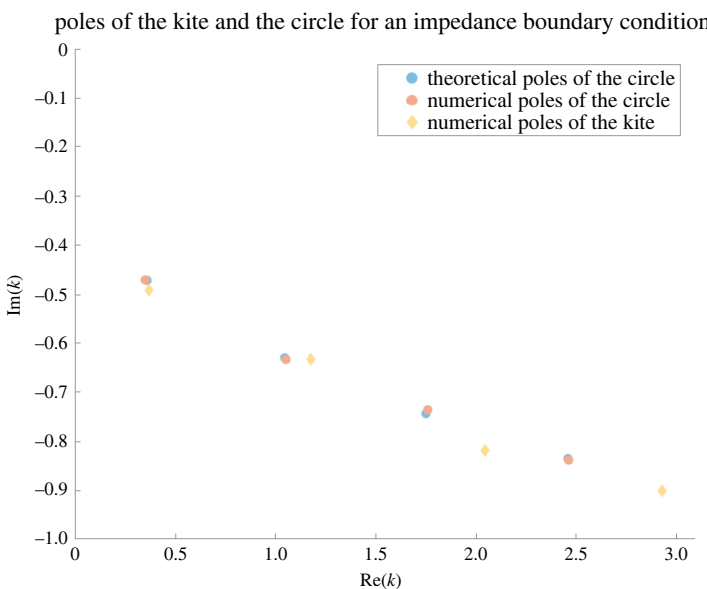


Figure 5. Poles of the impedance boundary problem for a kite and a circle.

a Neumann problem (η small), the imaginary part of the scattering pole is well approximated by the imaginary part of the Neumann pole. However, we refrain ourselves from drawing a general conclusion, since this observation is made on a single pole for a particular shape (the kite).

(d) The influence of continuous perturbations of the geometry

Next, we investigate the behaviour of a scattering pole for an impedance kite with $\eta = 0.1$, with respect to continuous perturbations of the shape. We consider a one-parametric family of kites with the equation

$$\mathcal{K}(\theta) = (\cos(\theta) + a \cdot \cos(2\theta) - a, 1.5 \sin(\theta)), \quad \theta \in [0; 2\pi],$$

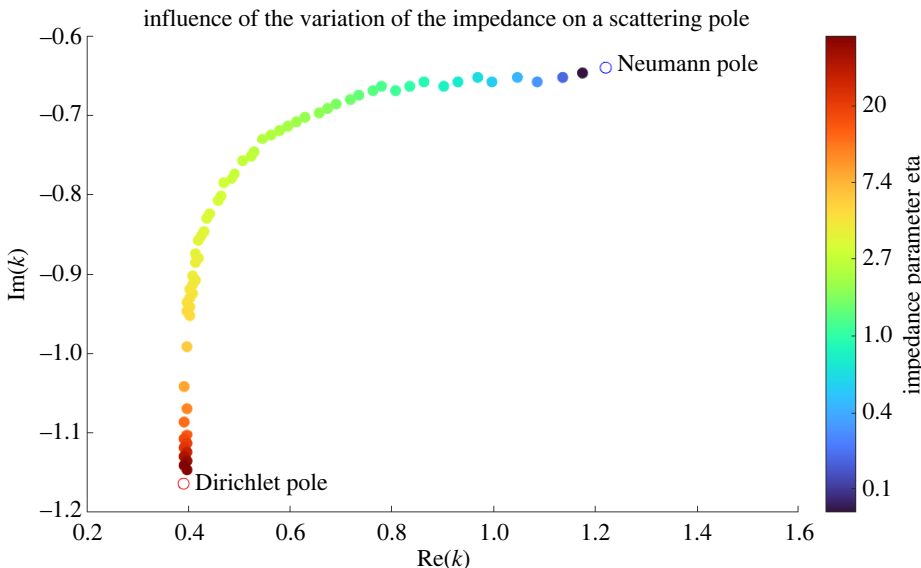


Figure 6. Tracing the change of a scattering pole in terms of η as it changes from zero (Dirichlet) to ∞ (Neumann).

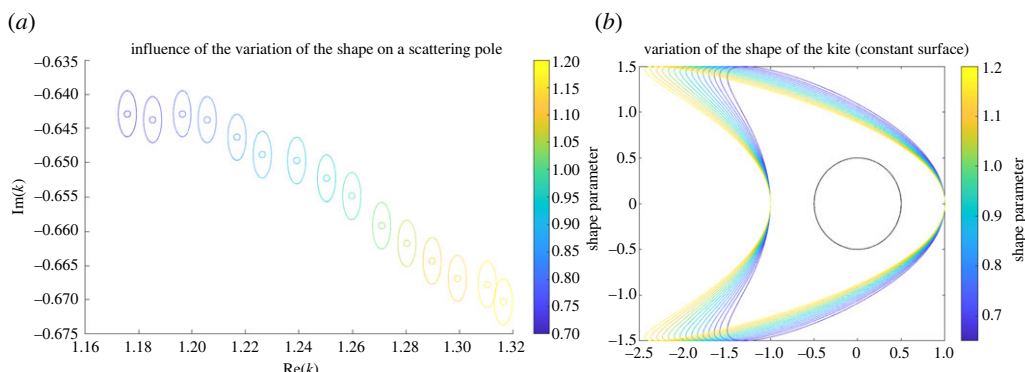


Figure 7. (a and b) Tracing the change of a scattering pole with respect to smooth surface preserving perturbation of the kite region with impedance boundary condition.

where a becomes the parameter. We numerically compute the surface of the kite and note that the area is invariant with respect to a . We then vary this parameter, and observe the shift of a scattering pole. The results are shown in figure 7, where a ranges from 0.6 to 1.2.

Once again we observe a continuous dependence of the scattering pole, this time with respect to this particular class of continuous perturbations of the shape of the object. For example, a change in the parameter of the shape going from 0.6 to 1.2, that is a 100% increase, is echoed in the scattering poles in a nonlinear fashion, with a 11% increase in the real part and 3% decrease in the imaginary part. The way the information about the shape is encoded in the scattering poles is not trivial, but could be exploited.

Of course, these numerical examples are preliminary and are meant as a proof of concept. Nevertheless, they show the viability of our numerical method. They also show that the scattering poles carry geometric and physical information about the scattering object.

Data accessibility. The user-friendly code with explanations, used for the computations of the examples presented in the paper, is posted on GitHub: (https://github.com/dana-zbbg/Scattering_Poles_Reconstruction) [28] and Zenodo: (<https://zenodo.org/records/11283655>) [29].

Declaration of AI use. We have not used AI-assisted technologies in creating this article.

Authors' contributions. F.C.: conceptualization, formal analysis, writing—review and editing; H.H.: conceptualization, formal analysis, writing—review and editing; D.Z.: formal analysis, software, writing—original draft.

All authors gave final approval for publication and agreed to be held accountable for the work performed therein.

Conflict of interest declaration. We declare we have no competing interests.

Funding. The research of F.C. is partially supported by the AFOSR grant no. FA9550-23-1-0256 and NSF grant no. DMS 2106255. The research of D.Z. is partially supported by the NSF grant no. DMS 2106255. The paper was completed while F.C. was visiting Isaac Newton Institute, University of Cambridge, UK as part of the programme 'Mathematical and Applications of Multiple Waves Scattering'.

References

1. Dyatlov S, Zworski M. 2019 *Mathematical theory of scattering resonances*. AMS Graduate Studies in Mathematics, no. 200. Providence, RI: American Mathematical Society.
2. Lax PD, Phillips RS. 1989 *Scattering theory*, 2nd edn. Pure and Applied Mathematics, Boston, MA: Academic Press, Inc.
3. Melrose RB. 1995 *Geometric scattering theory*. Cambridge, UK: Cambridge University Press.
4. Datchev K, Kang D, Kessler A. 2015 Non-trapping surfaces of revolution with long-living resonances. *Math. Res. Lett.* **22**, 23–42. ([doi:10.4310/MRL.2015.v22.n1.a3](https://doi.org/10.4310/MRL.2015.v22.n1.a3))
5. Labreuche C. 1999 Generalization of the Schwarz reflection principle in scattering theory for dissipative systems: application to purely imaginary resonant frequencies. *SIAM J. Math. Anal.* **30**, 848–878. ([doi:10.1137/S0036141997329214](https://doi.org/10.1137/S0036141997329214))
6. Labreuche C. 1998 Purely imaginary resonant frequencies for a lossy inhomogeneous medium. *SIAM J. Appl. Math.* **59**, 725–742. ([doi:10.1137/S0036139997328568](https://doi.org/10.1137/S0036139997328568))
7. Meklachi T, Moskow S, Schotland J. 2018 Asymptotic analysis of resonances of small volume high contrast linear and nonlinear scatterers. *J. Math. Phys.* **59**, 083502. ([doi:10.1063/1.5031032](https://doi.org/10.1063/1.5031032))
8. Osting B, Weinstein M. 2013 Long-lived scattering resonances and Bragg structures. *SIAM J. Appl. Math.* **73**, 827–852. ([doi:10.1137/110856228](https://doi.org/10.1137/110856228))
9. Stefanov P. 2006 Sharp upper bounds on the number of the scattering poles. *J. Funct. Anal.* **231**, 111–142. ([doi:10.1016/j.jfa.2005.07.007](https://doi.org/10.1016/j.jfa.2005.07.007))
10. Stefanov P. 1999 Quasimodes and resonances: sharp lower bounds. *Duke Math. J.* **99**, 75–92. ([doi:10.1215/S0012-7094-99-09903-9](https://doi.org/10.1215/S0012-7094-99-09903-9))
11. Zworski M. 1999 Dimension of the limit set and the density of resonances for convex co-compact hyperbolic surfaces. *Invent. Math.* **136**, 353–409. ([doi:10.1007/s002220050313](https://doi.org/10.1007/s002220050313))
12. Gopalakrishnan J, Moskow S, Santosa F. 2008 Asymptotic and numerical techniques for resonances of thin photonic structures. *SIAM J. Appl. Math.* **69**, 37–63. ([doi:10.1137/070701388](https://doi.org/10.1137/070701388))
13. Labreuche C. 1997 *Problèmes inversés en diffraction d'ondes basses sur la notion de résonance*. Diss. Paris 9.
14. Ma Y, Sun J. 2023 Computation of scattering poles using boundary integrals. *Appl. Math. Lett.* **146**, 108792. ([doi:10.1016/j.aml.2023.108792](https://doi.org/10.1016/j.aml.2023.108792))
15. Ralston J. 1972 Variation of the transmission coefficient and comparison theorems for the purely imaginary poles of the scattering matrix. *Commun. Pure Appl. Math.* **25**, 45–61. ([doi:10.1002/cpa.3160250105](https://doi.org/10.1002/cpa.3160250105))
16. Kohn R, Lu J, Schweizer B, Weinstein M. 2014 A variational perspective on cloaking by anomalous localized resonance. *Commun. Math. Phys.* **328**, 1–27. ([doi:10.1007/s00220-014-1943-y](https://doi.org/10.1007/s00220-014-1943-y))
17. Labreuche C. 1997 Inverse obstacle scattering problem based on resonant frequencies. *Lect. Notes Phys.* **486**, 169–185. ([doi:10.1007/BFb0105769](https://doi.org/10.1007/BFb0105769))
18. Labreuche C. 1998 Uniqueness and stability of the recovery of a sound soft obstacle from a knowledge of its scattering resonances. *Commun. Partial Differ. Equ.* **23**, 1719–1748. ([doi:10.1080/03605309808821398](https://doi.org/10.1080/03605309808821398))
19. Cakoni F, Colton D, Haddar H. 2023 *Inverse scattering theory and transmission eigenvalues*, 2nd edn. CBMS Series, no. 98. Philadelphia, PA: SIAM.

20. Cakoni F, Colton D, Haddar H. 2010 On the determination of Dirichlet and transmission eigenvalues from far field data. *Comptes Rendus Mathematique* **348**, 379–383. ([doi:10.1016/j.crma.2010.02.003](https://doi.org/10.1016/j.crma.2010.02.003))
21. Kirsch A, Lechleiter A. 2013 The inside-outside duality for scattering problems by inhomogeneous media. *Inverse Prob.* **29**, 104011. ([doi:10.1088/0266-5611/29/10/104011](https://doi.org/10.1088/0266-5611/29/10/104011))
22. Audibert L, Haddar H. 2014 A generalized formulation of the linear sampling method with exact characterization of targets in terms of farfield measurements. *Inverse Prob.* **30**, 035011. ([doi:10.1088/0266-5611/30/3/035011](https://doi.org/10.1088/0266-5611/30/3/035011))
23. Cakoni F, Colton D, Haddar H. 2020 A duality between scattering poles and transmission eigenvalues in scattering theory. *Proc. R. Soc. A* **476**, 20200612. ([doi:10.1098/rspa.2020.0612](https://doi.org/10.1098/rspa.2020.0612))
24. Colton D, Kress R. 2019 *Inverse acoustic and electromagnetic scattering theory*, 4th edn. Applied Mathematical Sciences, no. 93. New York, NY: Springer.
25. McLean W. 2000 *Strongly elliptic systems and boundary integral equations*. Cambridge, UK: Cambridge University Press.
26. Taylor M. 1996 *Partial differential equations. II. Qualitative studies of linear equations*. Applied Mathematical Sciences, no. 116. New York, NY: Springer.
27. Gypsilab, *open Matlab toolbox* <https://github.com/matthieuaustral/gypsilab>.
28. Cakoni F, Haddar H, Zilberberg D. 2024 An algorithm for computing scattering poles based on dual characterization to interior eigenvalues. GitHub repository. (https://github.com/dana-zbbg/Scattering_Poles_Reconstruction)
29. Cakoni F, Haddar H, Zilberberg D. 2024 An algorithm for computing scattering poles based on dual characterization to interior eigenvalues. Zenodo. (<https://zenodo.org/records/11283655>)